Supporting Information

Uniform distribution of post-synthetic linker exchange in metal-organic frameworks revealed by Rutherford Backscattering Spectrometry

Ulrike Fluch, Valentina Paneta, Daniel Primetzhofer, and Sascha Ott**

Table of Contents:

1 General remarks

2 RBS – Experimental set-up

3 Synthesis

3.1 UiO–66

3.2 UiO–66@Si

3.3 2–Iodoterephthalic acid

4 Ligand exchange and sample preparation for analysis

5 Physical measurements

5.1 NMR analysis of UiO–66 after PSE

5.2 RBS results

5.3 PXRD measurements

5.4 SEM measurements

6 References

The following abbreviations have been used throughout the supporting information:

bdc/I–bdc	Benzene-1,4-dicarboxylate/ Iodobenzene-1,4-dicarboxylate
MOF	Metal Organic Framework
MOF@Si	MOF grown on Silicon wafer
NMR	Nuclear Magnetic Resonance
PSE	Post-Synthetic linker Exchange
RBS	Rutherford Backscattering Spectrometry
PXRD	Powder X–Ray Diffraction
SEM	Scanning Electron Microscope
UiO	University of Oslo
SRIM	Software "The stopping and range of ions in matter"

1 General remarks

All purchased chemicals were used without further purification except where stated otherwise. DMF used for synthesizing UiO–66 was pre-dried over 4 Å molecular sieves. X–Ray powder diffraction patterns were collected using a Siemens D5000 utilizing a monochromatic Cu K_{α} radiation source at 40 kV, 40 mA for Cu Kα, (λ = 1.5406 Å) with a scan speed of 0.10 sec/step from 5 to 40º at a step size of 0.02º. NMR spectra were recorded on a JEOL Eclipse+ 400 MHz spectrometer. Chemical shifts are in parts per million using the residual protic solvent peak (Chloroform-*d*, DMSO-*d*6) as references. Scanning electron microscopy (SEM) was performed on a Zeiss 1550 with AZtec EDS equipped with InLens, SEII, and BSD detectors. The measurements were performed at 3 kV at working distances of 3.2 to 4.0 mm. The samples were sputtered prior to the measurements with a Polaron Sputter Coater (Au / Pd) for 40 seconds. p-Type silicon wafers with one polished side and a (100) orientation were cleaned in piranha acid prior to their use in the UiO–66 drop-casting procedure or for the UiO–66@Si synthesis.

2 RBS – Experimental set-up

The RBS experiments were performed employing the 5MV NEC 15SDH-2 Pelletron Tandem accelerator at the Ångström laboratory in Uppsala. Two different types of beam**s**, namely $^{4}He^{+}$ at 6 MeV and $^{12}C^{3+}$ at 11 MeV were used in the analys**e**s. The $^{12}C^{3+}$ beam provides enhanced depth resolution and superior mass separation for ^{nat}Zr and ^{127}I compared to the more conventional ^{4}He beam. The samples were transferred to a high-vacuum chamber with a base pressure of $1x10^{-7}$ mbar. The particle beam was collimated to a ~$1mm^{2}$ spot when directed under normal incidence on the targets. A 300 µm thick PIPS semiconductor detector was used to detect the energy of scattered primary particles in an angle of 170 degrees.

3 Synthesis

3.1 UiO–66

UiO–66 was synthesized according to literature procedures under solvothermal conditions using benzoic acid as a modulator[1]. After the syntheses, the powder MOFs were soaked once in fresh DMF, three times in fresh methanol and then stored in this solvent until further use.

3.2 UiO−66@Si

For the UiO–66@Si synthesis, silicon wafer pieces were cleaned in 80°C piranha acid for 30 minutes, washed with distilled water and blow-dried prior to use. The cleaned wafer pieces were placed in the

synthesis vials in a 45° angel with the polished side facing downwards to avoid precipitation and therefore multilayer formation. The conditions for the UiO–66@Si preparation were identical to those used for the bulk synthesis. UiO–66–(I–bdc)@Si was prepared by replacing bdc with I–bdc. After the solvothermal synthesis, the wafers were washed with DMF and soaked for 24 hours in fresh methanol three times. The wafers were stored in methanol until further use.

3.3 2–Iodoterephthalic acid

500 mg Dimethyl 2–iodoterephthalate (1 eq, 1.56 mmol) were dissolved in 30 ml of a THF/MeOH/H_2O (3/2/1) mixture. 5 eq LiOH (187 mg) were added and the reaction mixture was stirred at room temperature for 2 hours. The mixture was concentrated under reduced pressure. More water was added and the product was extracted with ethyl acetate tree times. The combined organic phases were washed with brine, dried over Na_2SO_4 before the solvent was removed under reduced pressure. The product was obtained as white to light yellow powder in quantitative yield.

4 Ligand exchange and sample preparation for analysis

For the exchange reaction on bulk UiO–66 powder, the MOF was dried under vacuum. For one set of 8 time points 80 mg bulk UiO–66 was used. The powder was suspended in 14 ml of a 40 mM methanolic solution of I–bdc (giving a I–bdc/bdc ratio of roughly 2:1), capped and incubated at room temperature. Samples (1 ml) of the agitated suspension were taken after 5, 15, 30, 45 and 60 minutes as well as after 3, 6 and 24 hours. The samples were centrifuged and the obtained pellets were re-suspended in fresh methanol and again centrifuged. This procedure was repeated at least eight times before the samples were dried. For the RBS analyses, 200 µl of suspensions with a concentration of 4 mg/ml methanol were made and drop casted onto cleaned silicon wafers.

For the PSE reactions on the UiO–66@Si samples, wafer pieces were placed in 3 ml of a 40 mM solution of I–bdc in methanol in a microwave vial. The exposure times were 5, 15, 30, 45, 60 seconds, 3, 6 and 24 hours, followed by thorough washing with methanol. Two replicates of each time point were made.

The preparation of the thyroxine samples involved the spin casting of methanolic solutions of L-thyroxine (1 mg in 1 ml), using a spin coater KW-4A of CHEMAT TECHNOLOGY INC. The spinning process was performed in two stages of different rotation speeds, firstly 1000 rpm for 12 sec to achieve proper wetting of the sample followed by an acceleration to 2000 rpm for 30 sec to form a sufficiently thin layer and remove excess material.

5 Physical measurements

5.1 NMR analysis of UiO–66 after PSE

For NMR analysis, 5 mg of bulk UiO–66 that had been exposed to PSE conditions were suspended in deuterated DMSO and dissolved by adding 5 µl of 48% HF solution. Figure S1 shows the ligand composition of the bulk UiO–66 samples before and after PSE for different durations of time. Benzoic acid which was the modulator during the solvothermal synthesis can be identified in the NMR spectra at δ = 7.50; 7.60; 7.93 ppm in addition to the expected signals from bdc (δ = 8.04 ppm) and I–bdc (δ = 7.70; 7.97; 8.40 ppm). It becomes evident from Figure S1 that the initial incorporation of I–bdc is accompanied with a decrease in benzoic acid content. After about 30 minutes, the concentration of benzoic acid stays constant and additional I**–**bdc is incorporated by replacing bdc in a PSE reaction.

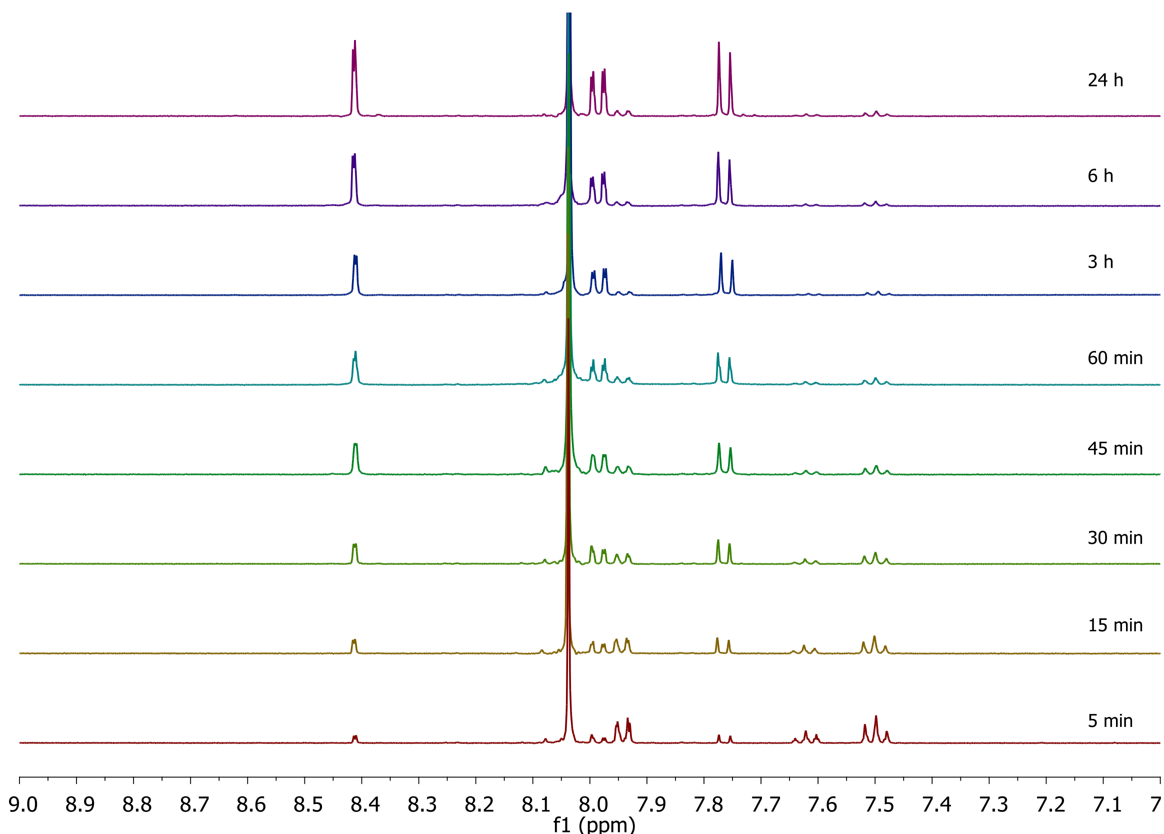

Figure S1. Stacked ^{1}H NMR of digested MOF samples at different PSE times. The spectra are normalized to the height of the bdc peak (8.04 ppm).

Example for the calculation of the I–bdc concentration by NMR

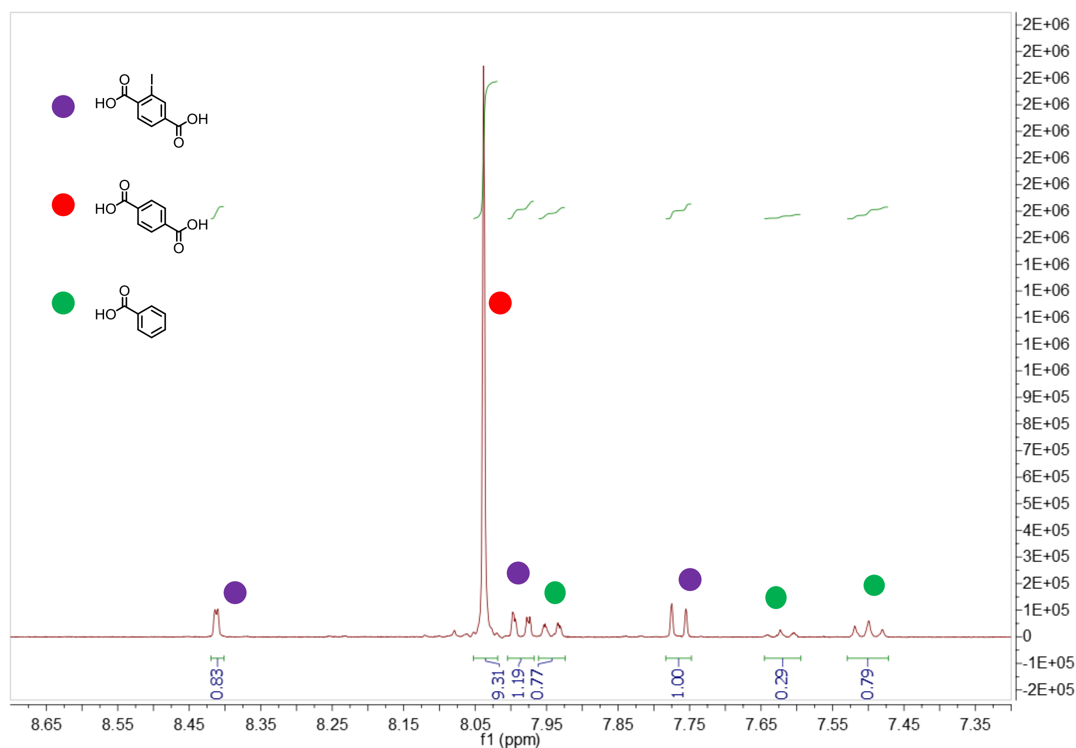

Figure S2. ^{1}H NMR of the digested MOF with a PSE time of 30 minutes. The colored dots represent the three different compounds found in the MOF. Violet is I–bdc, red: bdc and green: benzoic acid.

The calculation of the I–bdc concentration in the sample is exemplified for Figure S2 and summarized in Table 1. In short, one representative peak for each compound was chosen (I–bdc @7.75 ppm, bdc@8.04 ppm and benzoic acid @7.50 ppm). The integrals were normalized so that they represent one proton. In the example (Table 1) the sum of these normalized integrals is 3.72, giving a percentage of the I-bdc linker in the material of 1.00/3.72 = 27 %

Table 1. Representative peaks by NMR for the calculation of PSE amount.

ppm	Compound	# H's	Integral	Calculated for 1 H	% in MOF
8.04	bdc	4	9.31	2.33	63
7.75	I–bdc	1	1.00	1.00	27
7.50	Bz	2	0.79	0.39	10
∑				3.72	100

5.2 Rutherford Backscattering Spectrometry

Full spectrum

A typical spectrum acquired for 6 Mev alpha-particles scattered (detection angle 170°) from a bulk UiO-66 MOF sample with 1h PSE exposure time is shown in the following figure, indicating the Rutherford and the non-Rutherford scattering parts. The scattering cross sections for both Zr and I (including all isotopes) follow the Rutherford formula (hence RBS), while for the lighter elements comprising the sample (mainly Si, O, C), the cross section deviate from Rutherford in both magnitude and energy dependence and presents resonant structures. Note that the signals for all film constituents are limited to energies near the kinematic limit, whereas the Si-signal from the wafer substrate is present at all energies below $k \times E_0^{Si}$, as indicated by the arrows.

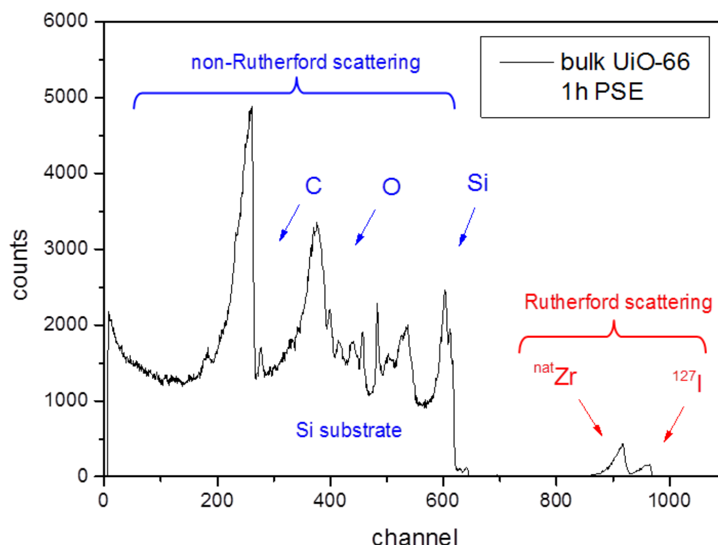

Figure S3. A typical spectrum acquired for 6 Mev alpha-particles scattered (detection angle 170°) from a bulk UiO-66 MOF sample with 1h PSE exposure time

Signal shapes

The origin of the different spectral shapes of the signals from Zr and I obtained in RBS is seen in the following figure. The spectrum presents a simulation of 6 MeV alpha particles scattered in an angle of 170° by natural Zr (5 isotopes) and I (monoisotopic element - ^{127}I) for a thin film with large thickness variation (best mimicking the MOF films within the limitations of the code) by using the SIMNRA package.

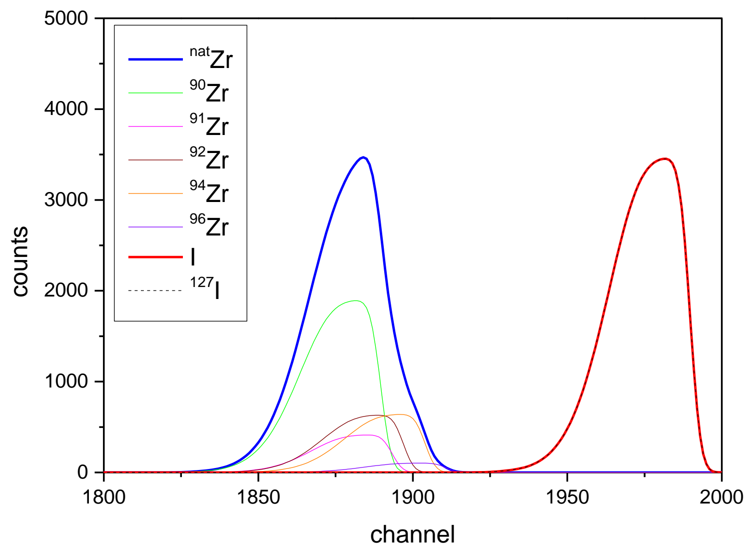

Figure S4. Simulation of 6 MeV alpha particles scattered in an angle of 170° by natural Zr (5 isotopes) and I (monoisotopic element - ^{127}I) for a thin film with large thickness variation

The following sketch is an example of a hexahedral cut from the view of the beam in terms of surface and deeper layers. As becomes apparent, for normal incidence and large scattering angles, trajectories with short path length (and thus small energy loss) will be overrepresented, explaining the observed shape of the signals in the spectra. Note that the present sketch is only one of many possible such visualizations, while the argument holds true also for other reasonable crystal geometries.

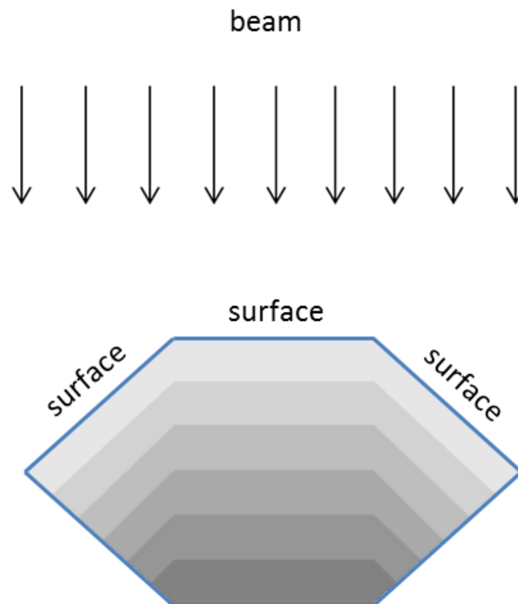

Figure S5. Sketch of a hexahedral cut from the view of the beam in terms of surface and deeper layers.

RBS depth profiling

The energy distribution of the detected particles can be converted to a depth scale of the sample as shown by the following formulas relating the energy loss (ΔE) with respect to the maximum possible energy due to scattering from the sample surface with the specific energy loss of the ions when crossing the target material. This energy loss per path length of the beam particles inside the material (defined as the stopping power S=dE/dx) is calculated for crossing the material before and after the scattering point (in- and outward path). The stopping cross section ε, is defined as the energy loss per atom per unit area (areal density N) of material traversed, as seen below. This representation is commonly made due to its independence of the density of the target material. The values of ion stopping cross sections are well known for MeV ions and can be found in SRIM.[2]

$$S \equiv \frac{dE}{dx} = N\varepsilon$$

For normal beam incidence and detection angle at 170°, the energy distribution ΔE of detected particles scattered from the surface till depth x is given by the following equations, while, depending on the nucleus that scatters the beam particles, a different kinematic factor (K) accounting for the energy loss in the elastic backscattering collision with a target nucleus needs to be taken into account. A more extensive description of the relation between energy loss, stopping cross sections and target thickness can be found in e.g reference [3].

$$\Delta E = [\varepsilon]Nx$$

$$[\varepsilon] = \left[K\varepsilon_{in} + \frac{1}{cos170^{\circ}}\varepsilon_{out}\right]$$

Stopping cross sections ε are dependent on the target composition and the particle energy. The small impact of the different iodine content in MOFs with different PSE exposure time on the stopping cross sections can be considered negligible to the total uncertainty of the depth scaling, when expressing depth in units of µm and not areal thickness (atoms/cm^2). The main source of uncertainty for the depth scaling

in µm is the adopted density values. Note, however, that a possible uncertainty in density on the order of 10% will result only in a linear scaling factor and consequently a relative comparison of the spectra is by far more accurate. In light of this, also the non-linear-dependence of the stopping on the particle energy is considered to be negligible for the present thin films studied.

Remarks to the calculation of PSE yield by RBS:

The I–bdc concentrations relative to the Zr concentrations in the samples were taken from the RBS spectra by normalizing the signals by their respective cross sections (scattering probability of the different nuclei). The ratio of the two signals gives directly the I–bdt:Zr ratio, and thus the I–bdt concentration.

RBS response for drop-cast UiO–66 bulk samples vs. UiO–66@Si films:

Shown is the much broader response in the drop-casted UiO–66 samples due to poorly defined surface coverage with agglomerates, as compared to the well-defined, single-crystal layer in the UiO–66@Si films.

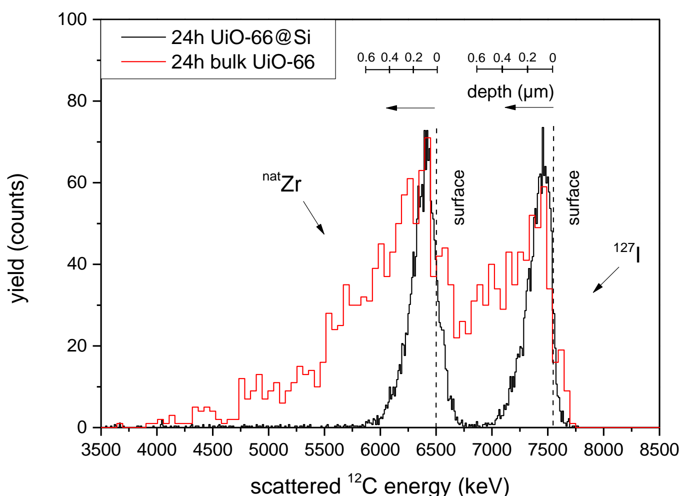

Figure S6. Yield of scattered C ions as a function of detected energies for scattering from bulk UiO–66 drop-casted on Si, and UiO–66@Si that had been exposed to PSE conditions with I–bdc for 24 h each. Visible is the broader RBS signals of the drop-casted bulk samples due to the poorly defined drop-casted films with MOF agglomeration. Note that the normalization of the Zr-signal is for convenience only and without a real physical meaning since the height of the signal is affected by the sample coverage which is lower in the case of UiO–66@Si.

5.3 PXRD measurements

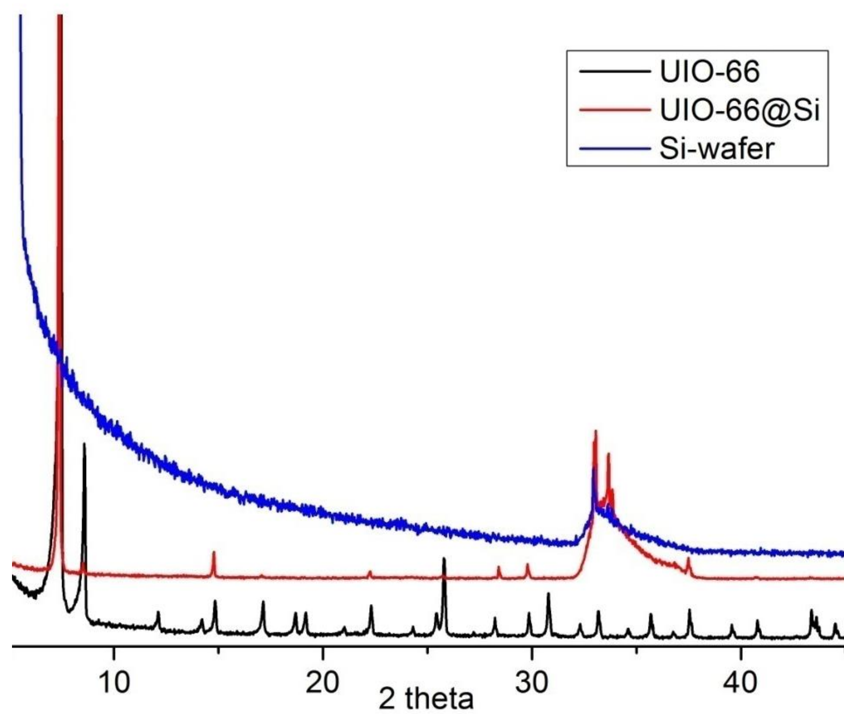

Figure S7. Stacked PXRD pattern of UIO–66 samples on wafer. Black powder sample UIO–66; red UIO–66 grown on Si–wafer growing with preference in (111) phase; blue clean Si–wafer.

5.4 SEM measurements

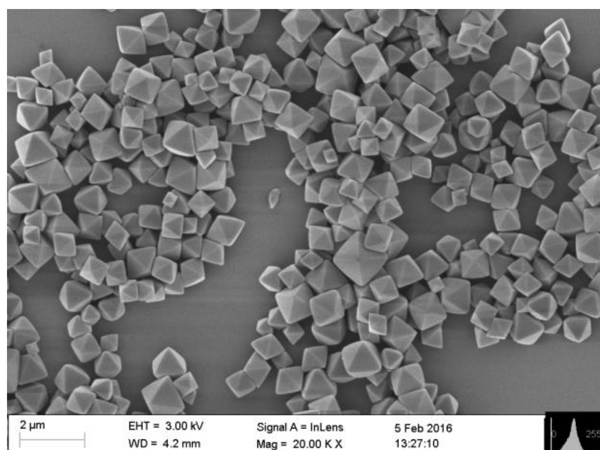

Figure S8. SEM image of drop-casted UiO-66 sample that was exposed to PSE conditions for 24 h.

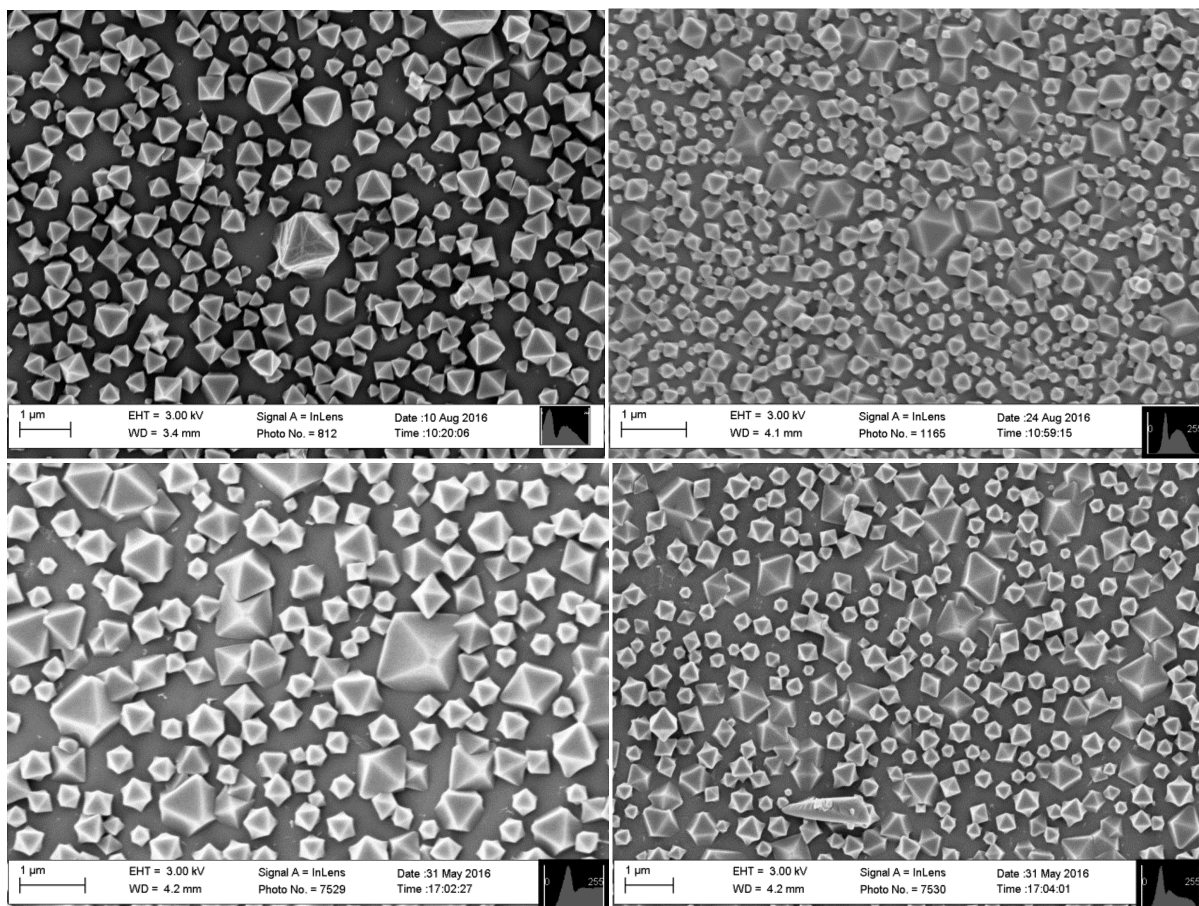

Figure S9. SEM image of UIO–66@Si before PSE (top left) and after 24 h PSE (top right), after 6 h PSE before (bottom left) and after the RBS study (bottom right). The scale bar indicates 1 µm. Different size of the crystals is due to different samples. Au/Pd sputtered samples cannot be used for PSE nor for RBS.

By looking at the samples by SEM no changes in the morphology of the crystals could be found. The size of the crystals as well as the coverage of the wafers vary from sample to sample, but the morphology of the samples before and after PSE, as well as before and after the RBS is identical. It is noteworthy that UiO–66 seems to grow on silicon wafers with a high preference in one phase presenting one triangle face parallel to the wafer surface. This behavior is consistent with the PXRD pattern of UiO–66@Si (Fig. S4) in which some reflections of the UiO–66 bulk pattern are missing. In comparing with literature data, the main peaks of UiO–66@Si show that this MOF grows on silicon with a preference for the (111) phase.[4]

6 References

(1) Schaate, A.; Roy, P.; Godt, A.; Lippke, J.; Waltz, F.; Wiebcke, M.; Behrens, P. *Chem. – Eur. J.* **2011**, *17* (24), 6643–6651.

(2) Ziegler, J.F.; Ziegler, M.D.; Biersack, J.P., *Nucl. Instr. And Methods B* **2010**, 268, 1818–1823.

(3) Wang, Y. Nastasi, M. A. Eds., *Handbook of modern ion beam materials analysis*, Materials Research Society, Warrendale, PA, 2nd ed., **2009**.

(4) Hinterholzinger, F. M.; Wuttke, S.; Roy, P.; Preuße, T.; Schaate, A.; Behrens, P.; Godt, A.; Bein, T. *Dalton Trans.* **2012**, *41* (14), 3899–3901.